Cryogenics in Space and the Cosmic Background Explorer (COBE)

Rainer Weiss, MIT

Hamilton Symposium

March 19, 2002

Louisiana State University

COSMOLOGICAL BACKGROUND RADIATION SATELLITE

J. Mather
P. Thaddeus
Goddard Institute for Space Studies

R. Weiss
D. Muehlner
Massachusetts Institute of Technology

D. T. Wilkinson
Princeton University

M. G. Hauser
R. F. Silverberg
Goddard Space Flight Center

OCTOBER 1974

B. Objectives and Significant Aspects

An Explorer spacecraft equipped with cryogenically cooled instrumentation will provide a uniquely sensitive system for study of diffuse cosmic radiation. It is proposed to develop a mission in which such a system is used to make definitive measurements on the radiative relics of the earliest stages of the universe. Four experiments are proposed, characterized by their common cosmological motivation and by compatible and relatively modest demands upon the spacecraft. The experiments proposed here include:

1. Spectrum of the 2.7 K Cosmic Background from 0.1 to 3 mm
2. Isotropy of the 2.7 K Cosmic Background between 0.5 and 3 mm Wavelength
3. Isotropy of the 2.7 K Cosmic Background at 3, 5, 9, and 16 mm Wavelength
4. Search for Diffuse Cosmic Radiation at 5-30 micron Wavelength.

The personnel responsible for each experiment and principal requirements for each are summarized in Table 1. It should be noted that experiment (3) does not require cryogenic cooling, but it is intimately related to the first two experiments, and does require a satellite platform for high quality results.

Advances in Cryogenic Engineering
Vol 16 , p277 (1972)

G—1

A SUPERFLUID PLUG FOR SPACE*

P. M. Selzer, W. M. Fairbank, and C. W. F. Everitt

Stanford University
Stanford, California

INTRODUCTION

This experiment is concerned with the problem of containing liquid helium in space. On earth, one maintains cryogenic equipment at 4°K by immersing it in liquid helium and utilizing the latent heat of the liquid to dissipate any heat input. Gravitational phase separation allows the boil-off gas to be withdrawn at the top of the dewar. Two major problems arise in a zero-g environment. First, we no longer may have an open gas-evacuation line because liquid will also be withdrawn. Second, there may not always be enough liquid in contact with the equipment to dissipate the entire heat input; consequently, the temperature of the system will rise.

In order to overcome these difficulties without spinning or using cumbersome electrostatic techniques, the use of a high thermal-conductivity porous plug is proposed which will operate in the superfluid regime. Liquid will flow through the plug in a controlled manner as discussed below. The exit channel will be evacuated in order to evaporate the liquid at its outer surface. With a plug of high thermal conductivity, the major portion of the heat needed to evaporate the liquid will be conducted from inside the chamber, while the high effective thermal conductivity of the superfluid film, which coats all inner surfaces, establishes thermal equilibrium throughout the dewar. Preliminary calculations suggest that this film will be several orders of magnitude thicker in space than on earth, thereby conducting ample amounts of liquid to the plug and providing adequate liquid contact with the equipment. (On earth, a wick must be used to provide the plug with enough fluid).

THEORY

Equations for describing superfluid flow through the plug may be derived from the equation of motion [1]

$$\frac{dv_s}{dt} = -\nabla G \tag{1}$$

or

$$\frac{dv_s}{dt} = S\nabla T - \frac{\nabla P}{\rho} + \frac{\rho_n}{2\rho}\nabla(v_n - v_s)^2 \tag{2}$$

* Work supported in part by NASA Grant No. NGR-05-020-019.

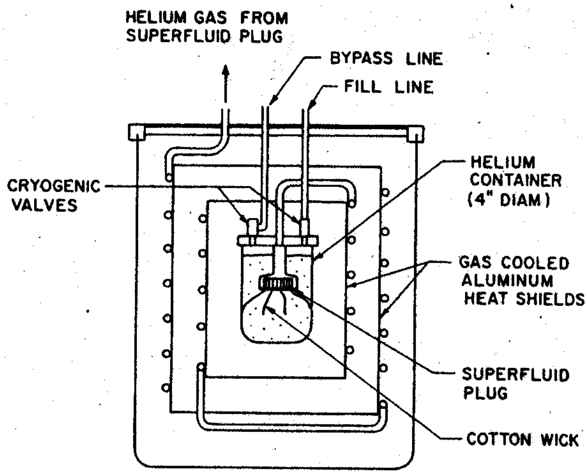

Fig. 1. Invertible dewar.

In order to test the plug, a dewar has been built which is designed to operate in any spatial orientation, including upside-down (see Fig. 1). If the refrigeration system is operable under negative-*g* conditions, there is good reason to believe that it can operate in zero-*g* as well. This dewar consists of a liquid-helium chamber with the plug inside. Two cryogenic valves, operated from above, are situated on top of the chamber for transfer of the liquid and by-passing the plug. Gas which leaves the plug is conducted through two aluminum heat shields before exiting at the top. The chamber and shields are wrapped with NRC superinsulation and placed inside an outer aluminum can which is subsequently evacuated to 10^{-6} torr.

To date, the dewar has been operated upright at 1.75°K and inverted at 2.28°K (above T_λ) for extended periods of time. A small modification must be made in one of the valves before the dewar can operate upside-down in the superfluid regime.

CONCLUSION

Using a superfluid plug promises to be an excellent method for containing liquid helium in space and provides a controlled flow of liquid below the λ point. By enlarging the plug to pass normal fluid as well, we have a system which is operable through a larger range of temperature with no chance of explosion. The use of a high thermal-conductivity plug should also be adaptable to the containment of other cryogenic fluids in a zero-*g* environment, provided adequate thermal equilibrium inside the dewar can be maintained.

NOTATION

A = total cross-sectional area of channels
A' = total cross-sectional area of metallic portion of plug
C = thermal conductance of metallic portion of plug
G = Gibbs potential
k = thermal conductivity
L = latent heat
$\dot{m}$ = mass flow rate
P = pressure
ΔP = pressure difference across plug
S = specific entropy

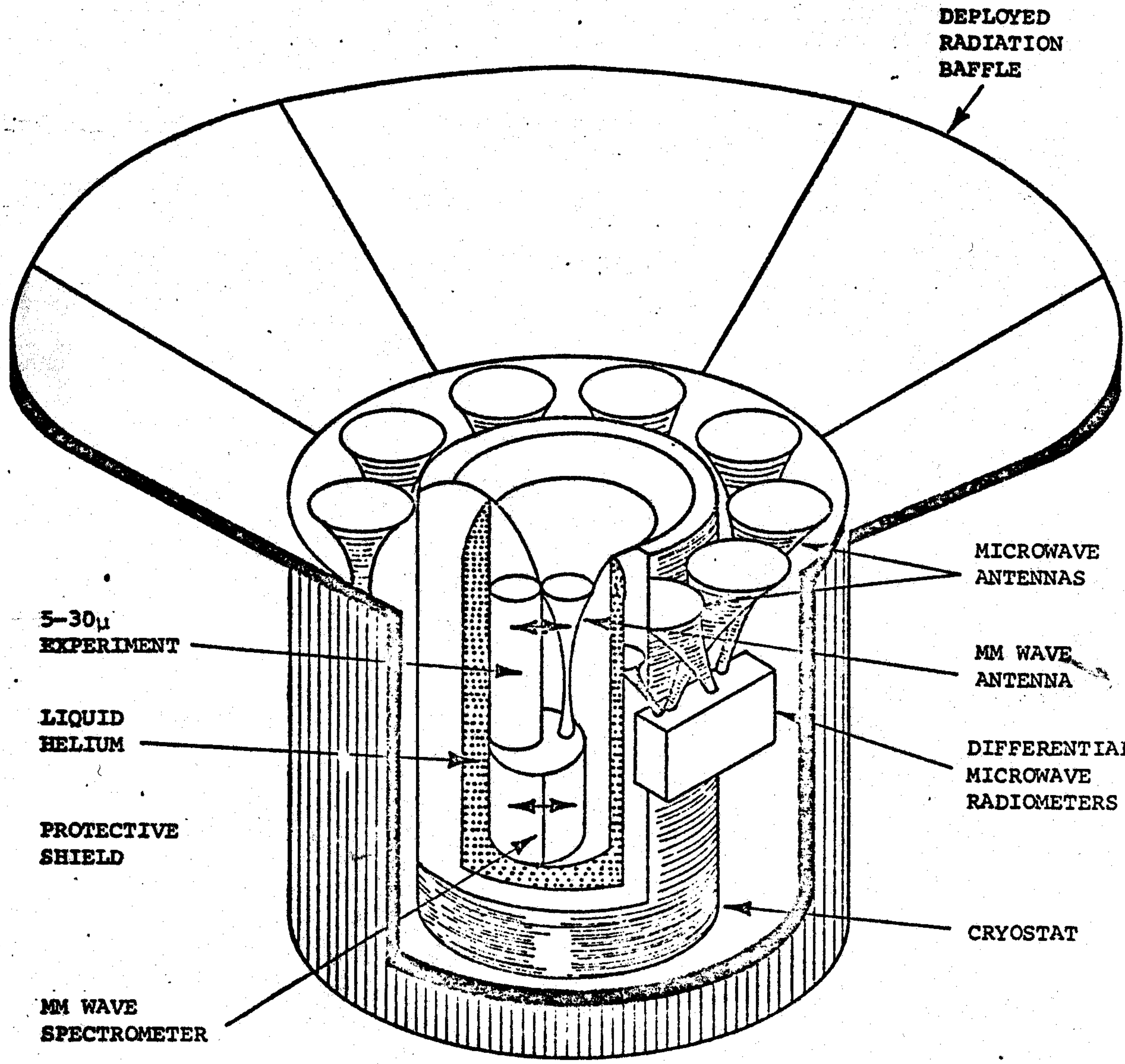

ARRANGEMENT OF EXPERIMENTS

TWO HELIUM COOLED EXPERIMENTS
TIME-SHARE THE APERTURE IN THIS VERSION

INSTRUMENT ARRANGEMENT ON PROPOSED SPACECRAFT

FIGURE 1

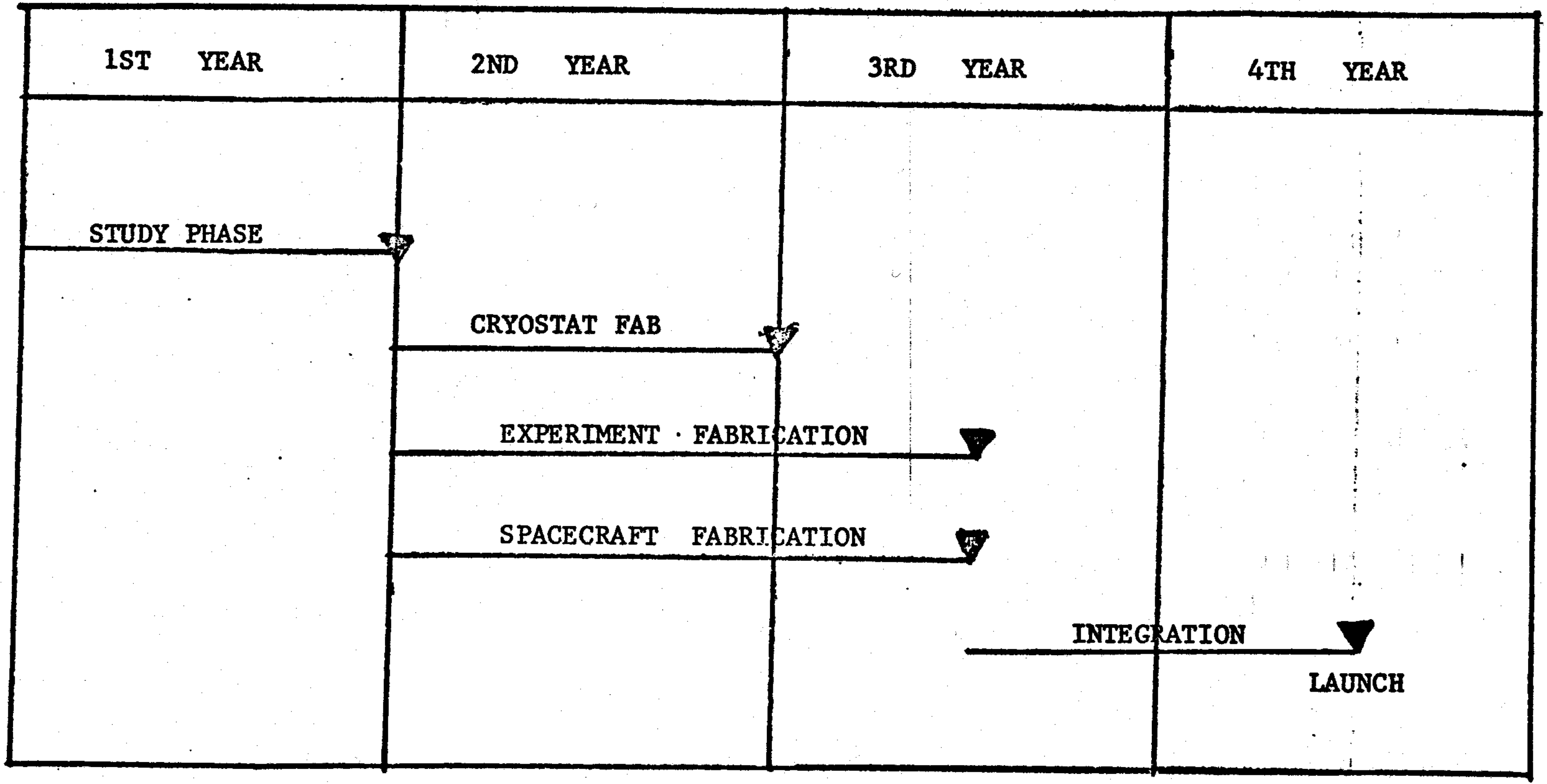

SCHEDULE FOR PROPOSED MISSION

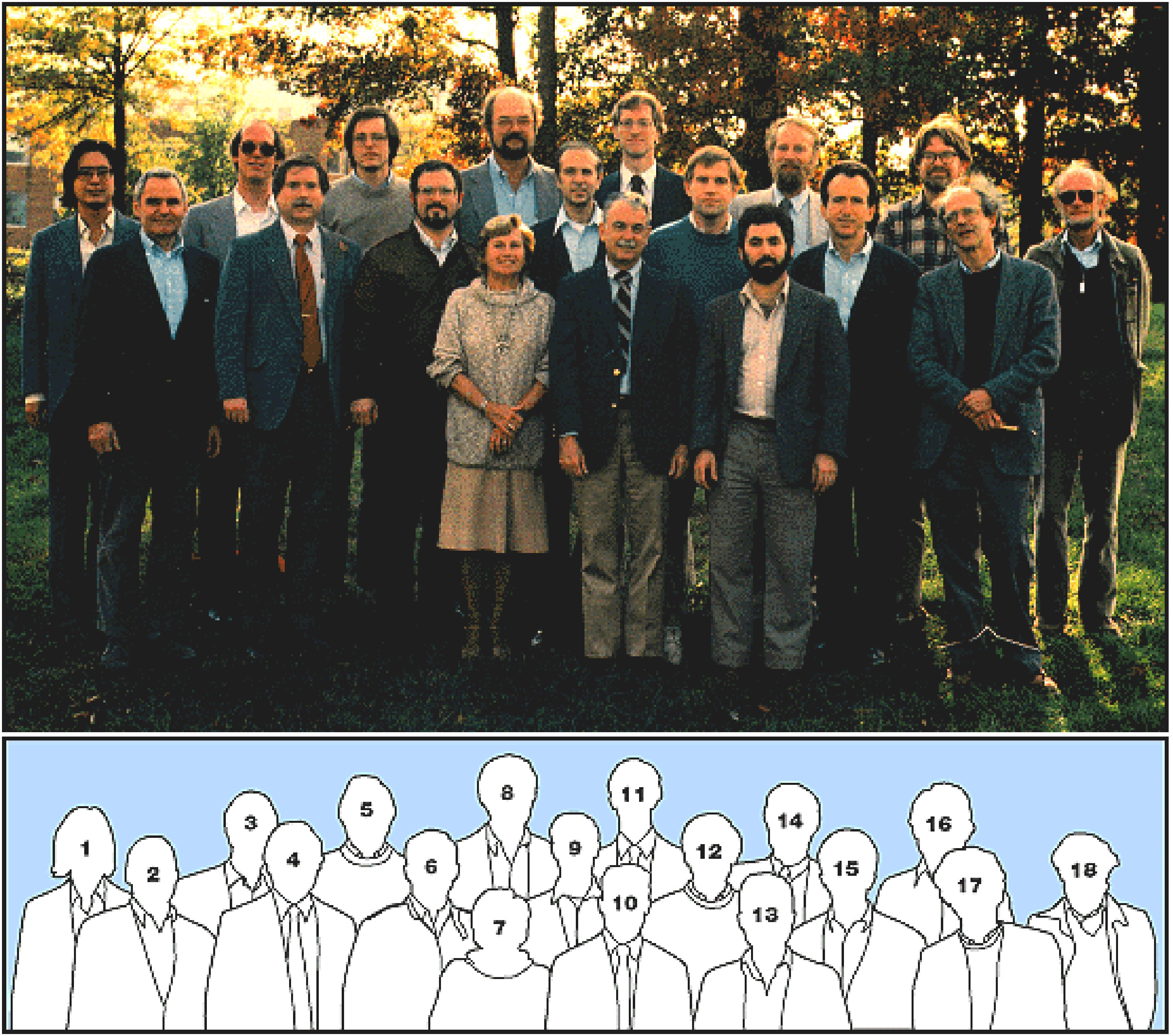
1
2
3
4
5
6
7
8
9
10
11
12
13
14
15
16
17
18

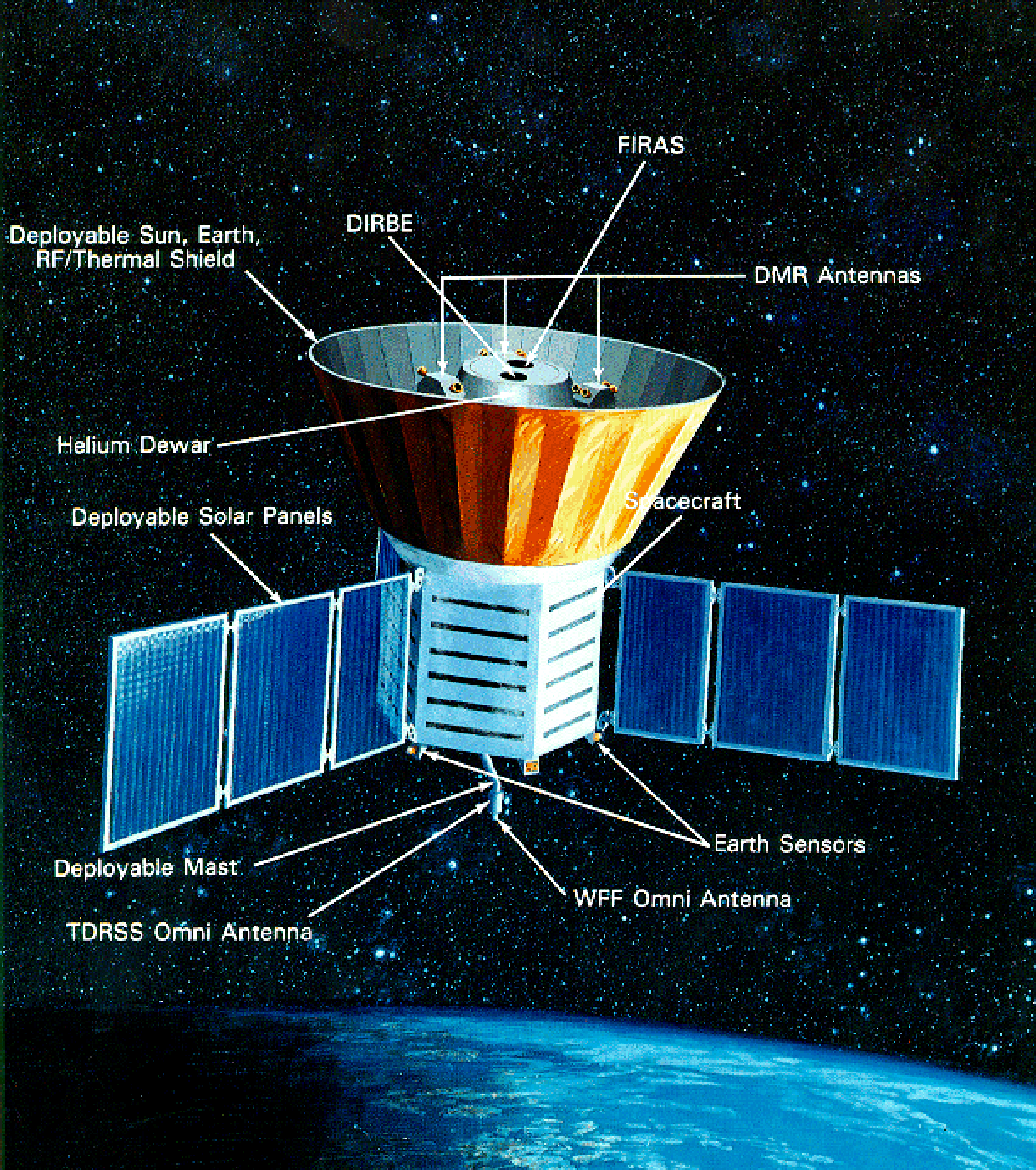
FIRAS
DIRBE
Deployable Sun, Earth,
RF/Thermal Shield
DMR Antennas
Helium Dewar
Spacecraft
Deployable Solar Panels
Earth Sensors
Deployable Mast
WFF Omni Antenna
TDRSS Omni Antenna

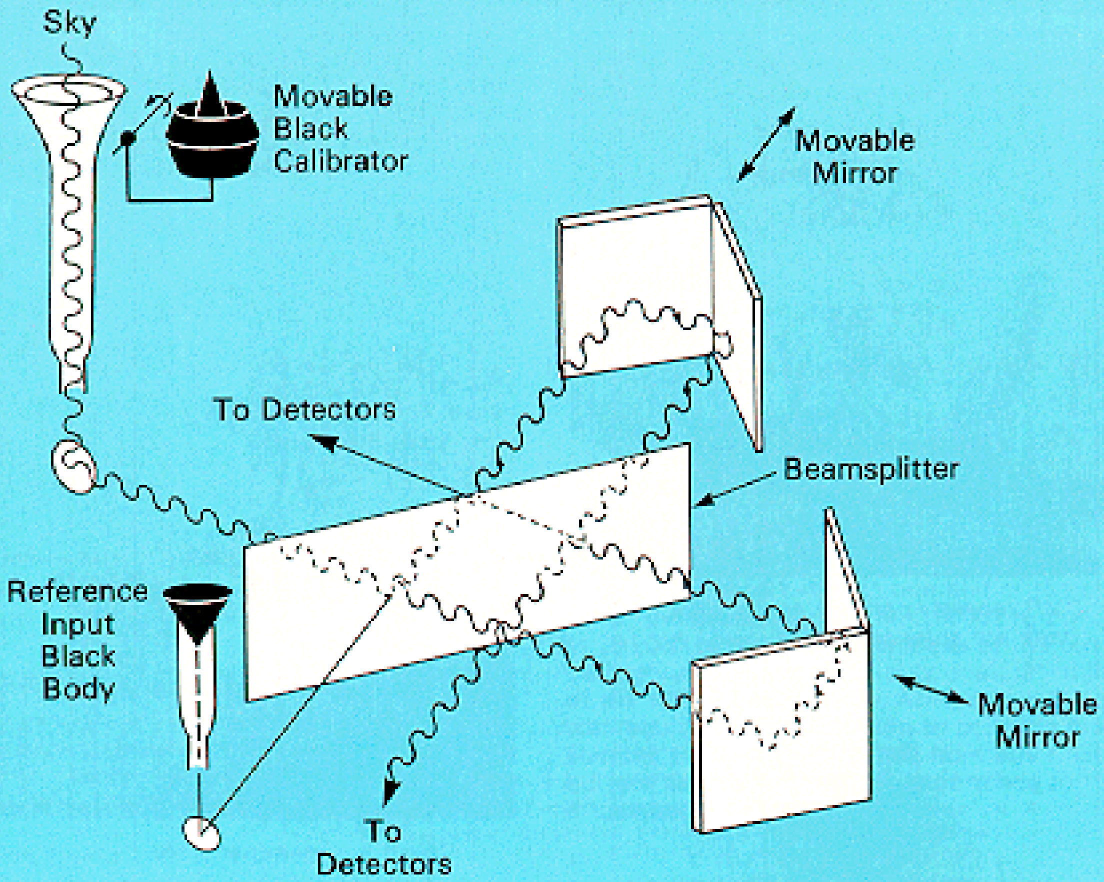
Sky
Movable Black Calibrator
Movable Mirror
To Detectors
Beamsplitter
Reference Input Black Body
Movable Mirror
To Detectors

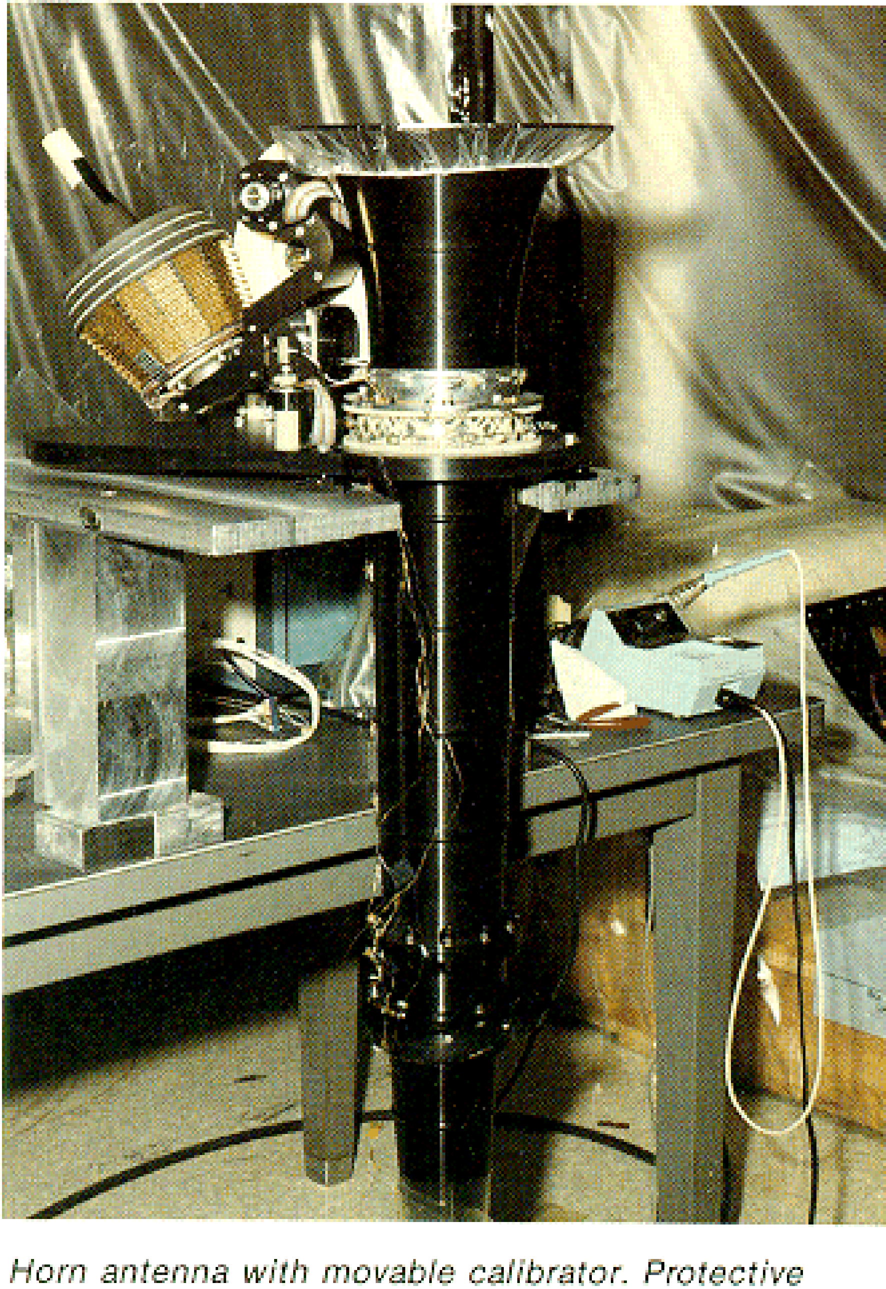

Horn antenna with movable calibrator. Protective plastic covers will be removed.

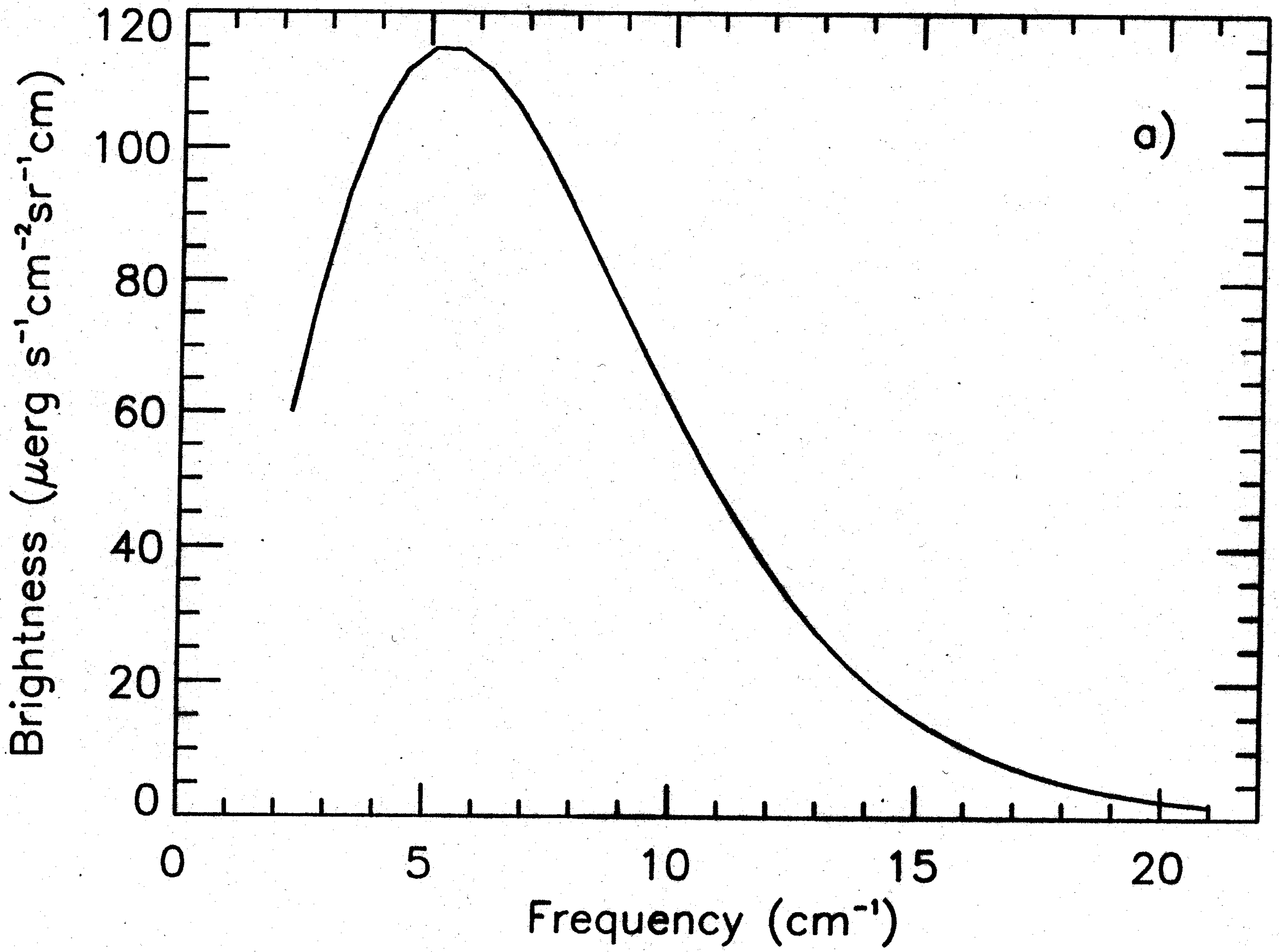

Brightness (μerg s⁻¹cm⁻²sr⁻¹cm)
Frequency (cm⁻¹)
a)
0
20
40
60
80
100
120
0
5
10
15
20

COBE Slide 37

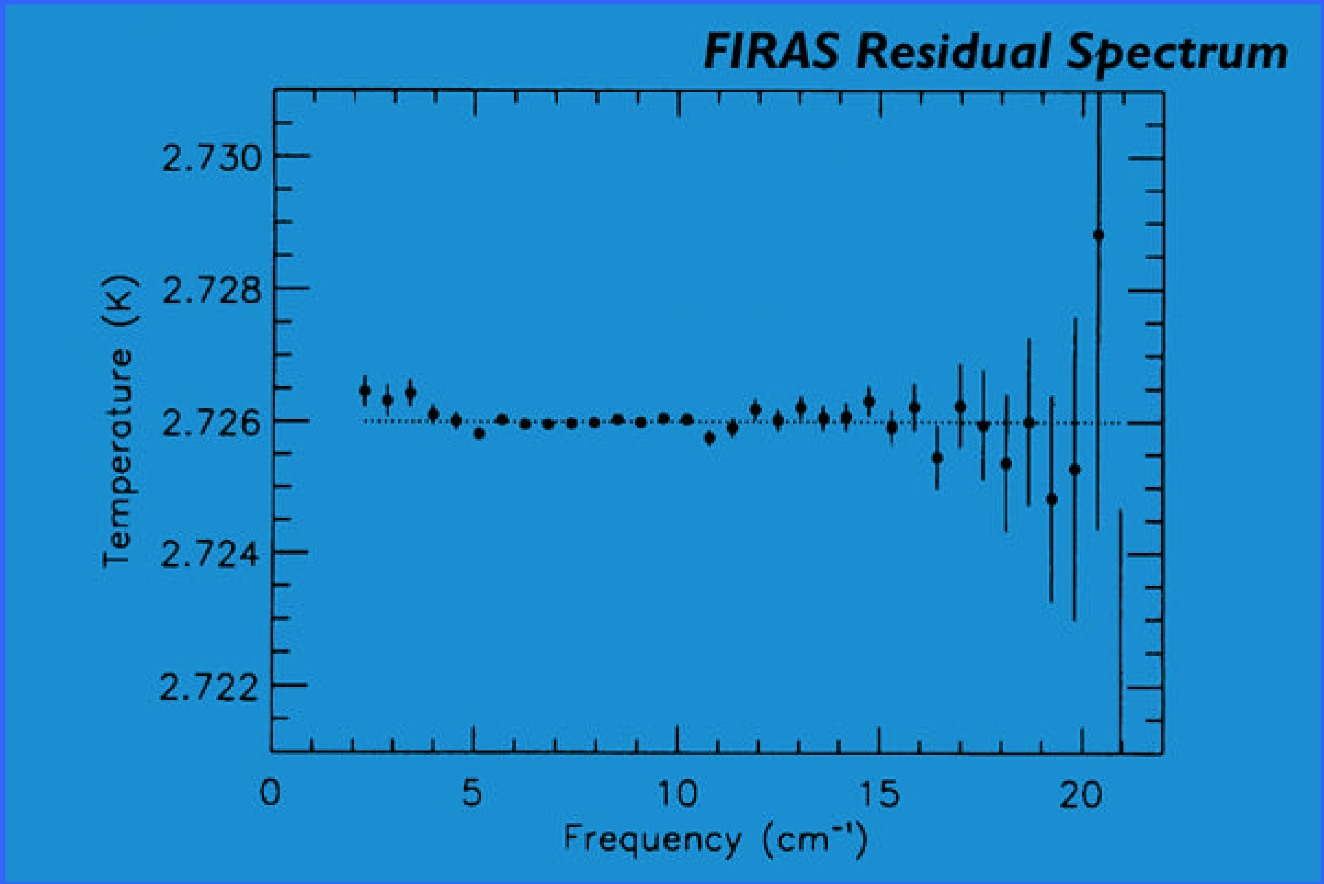

FIRAS measured cosmic microwave background radiation residual spectrum from Mather et al. 1994, ApJ, 420, 439. A Planck blackbody spectrum and a small Galactic emission component have been subtracted from the measured spectrum in order to make the residuals visible. To a very good approximation, the cosmic microwave background spectrum is the same as that of a 2.728 (+/- 0.004) degree Kelvin blackbody.

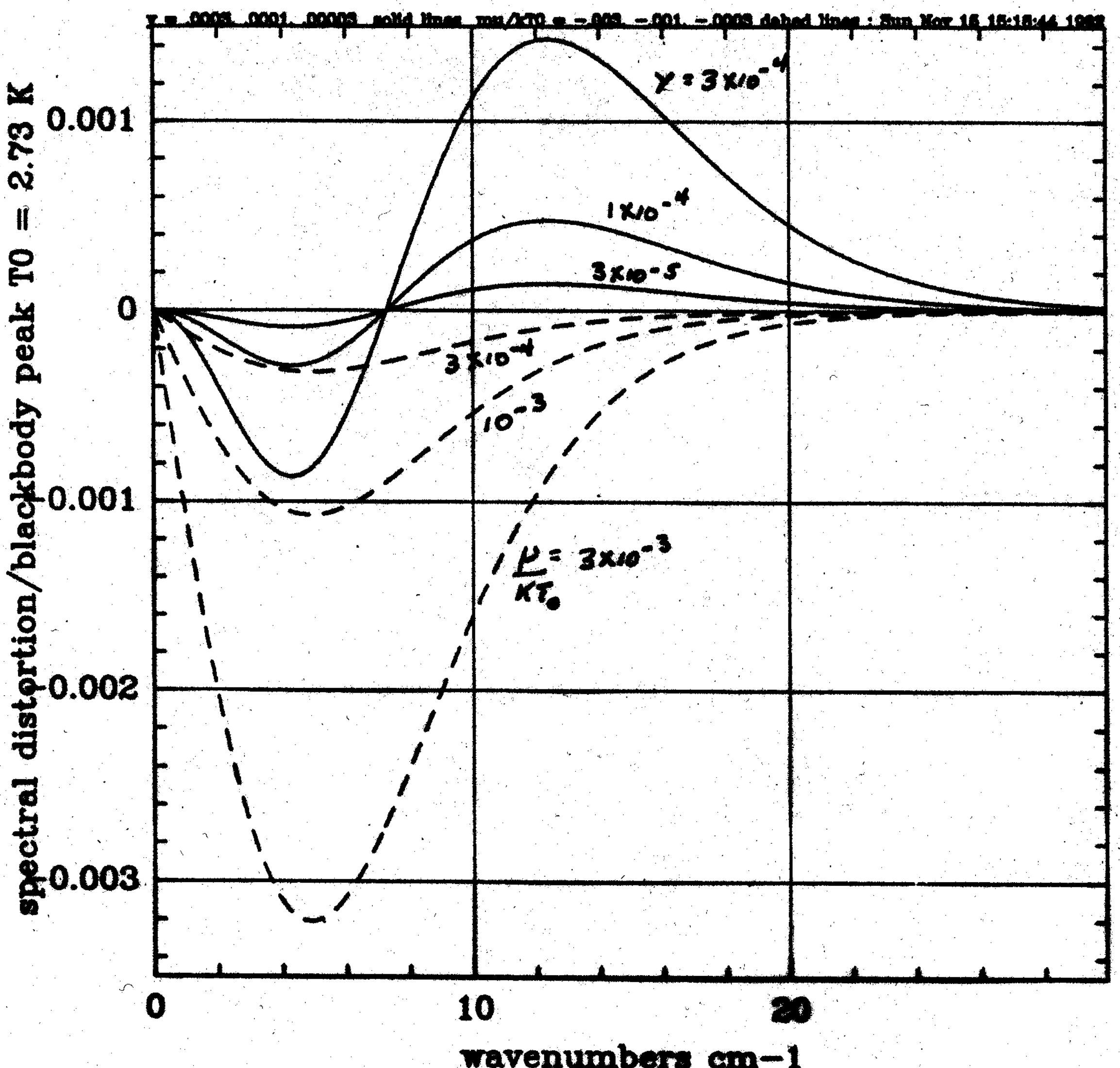

COMPTONIZATION

$$B(\nu, T') = \frac{2h\nu^3}{c^2} \frac{1}{e^{h\nu/kT'} - 1}$$

$$T' = T_0\left(1 + y\left(\frac{x(1+e^{-x})}{1-e^{-x}} - 4\right)\right) \qquad x = \frac{h\nu}{kT_0}$$

RELEASE OF LATENT HEAT

$$B(\nu, T) = \frac{2h\nu^3}{c^2} \frac{1}{e^{\frac{h\nu - \mu}{kT}} - 1}$$

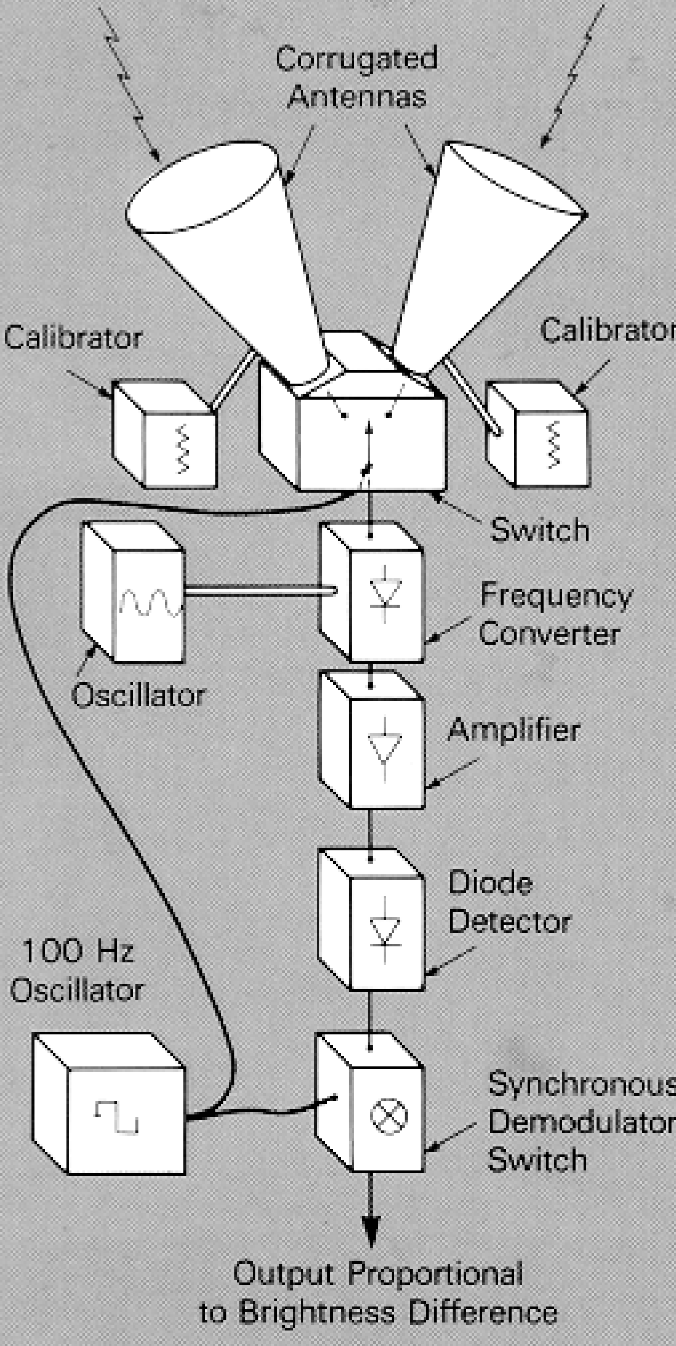

Corrugated
Antennas
Calibrator
Calibrator
Switch
Frequency
Converter
Oscillator
Amplifier
Diode
Detector
100 Hz
Oscillator
Synchronous
Demodulator
Switch
Output Proportional
to Brightness Difference

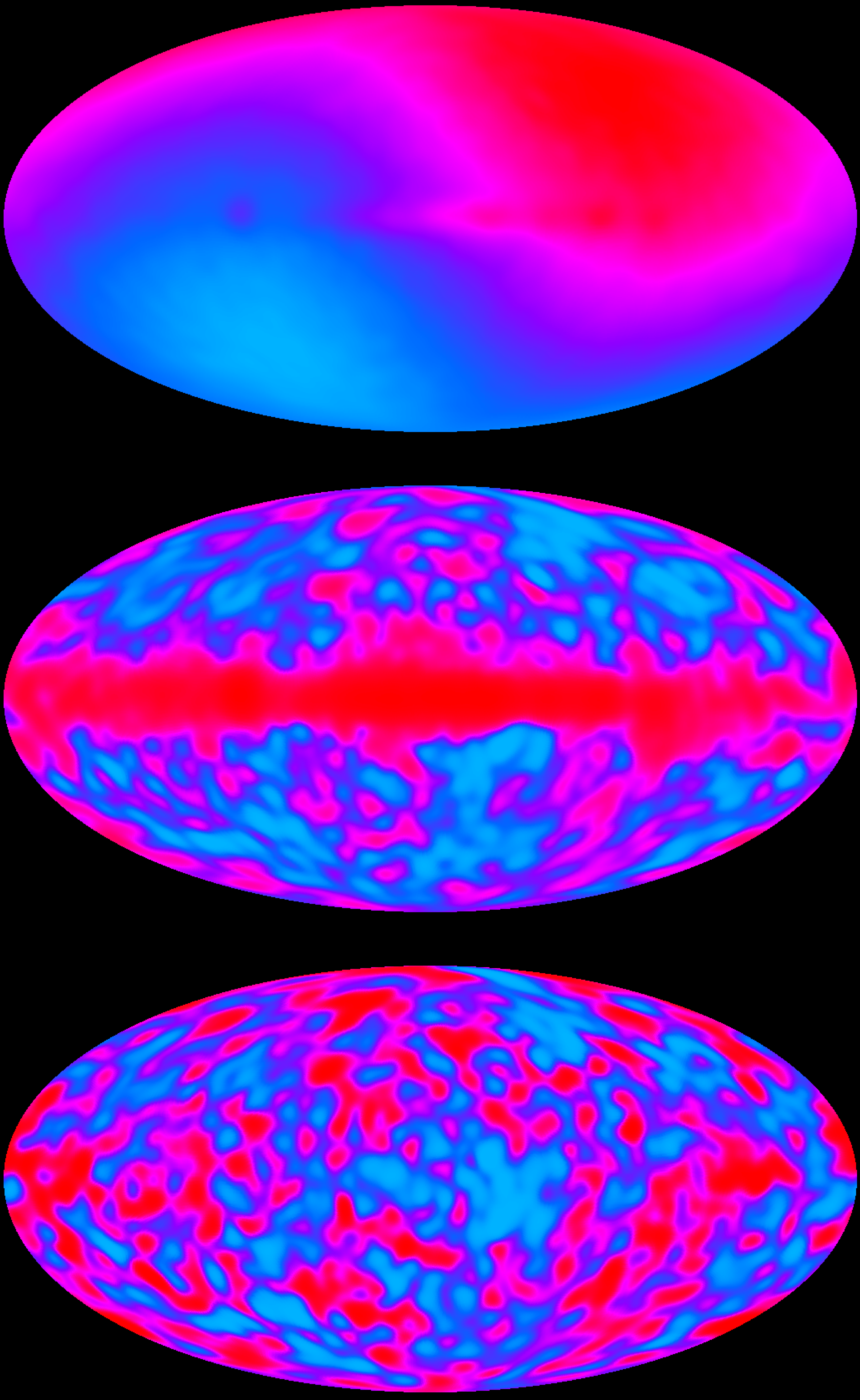

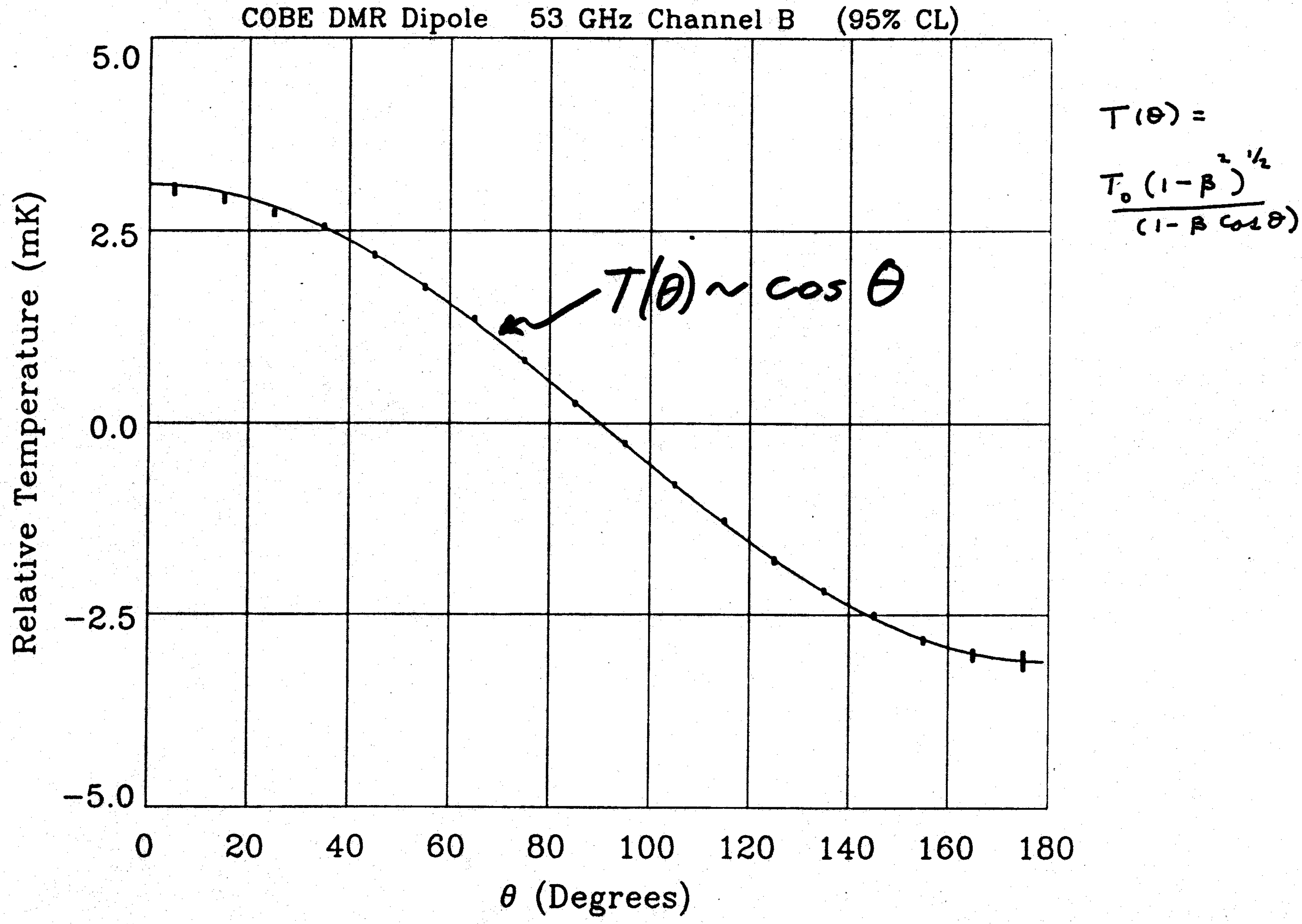

COBE DMR Dipole 53 GHz Channel B (95% CL)
Relative Temperature (mK)
5.0
2.5
0.0
−2.5
−5.0
0
20
40
60
80
100
120
140
160
180
θ (Degrees)
T(θ) ~ cos θ
T(θ) =
T₀ (1 − β²)^½ / (1 − β cos θ)

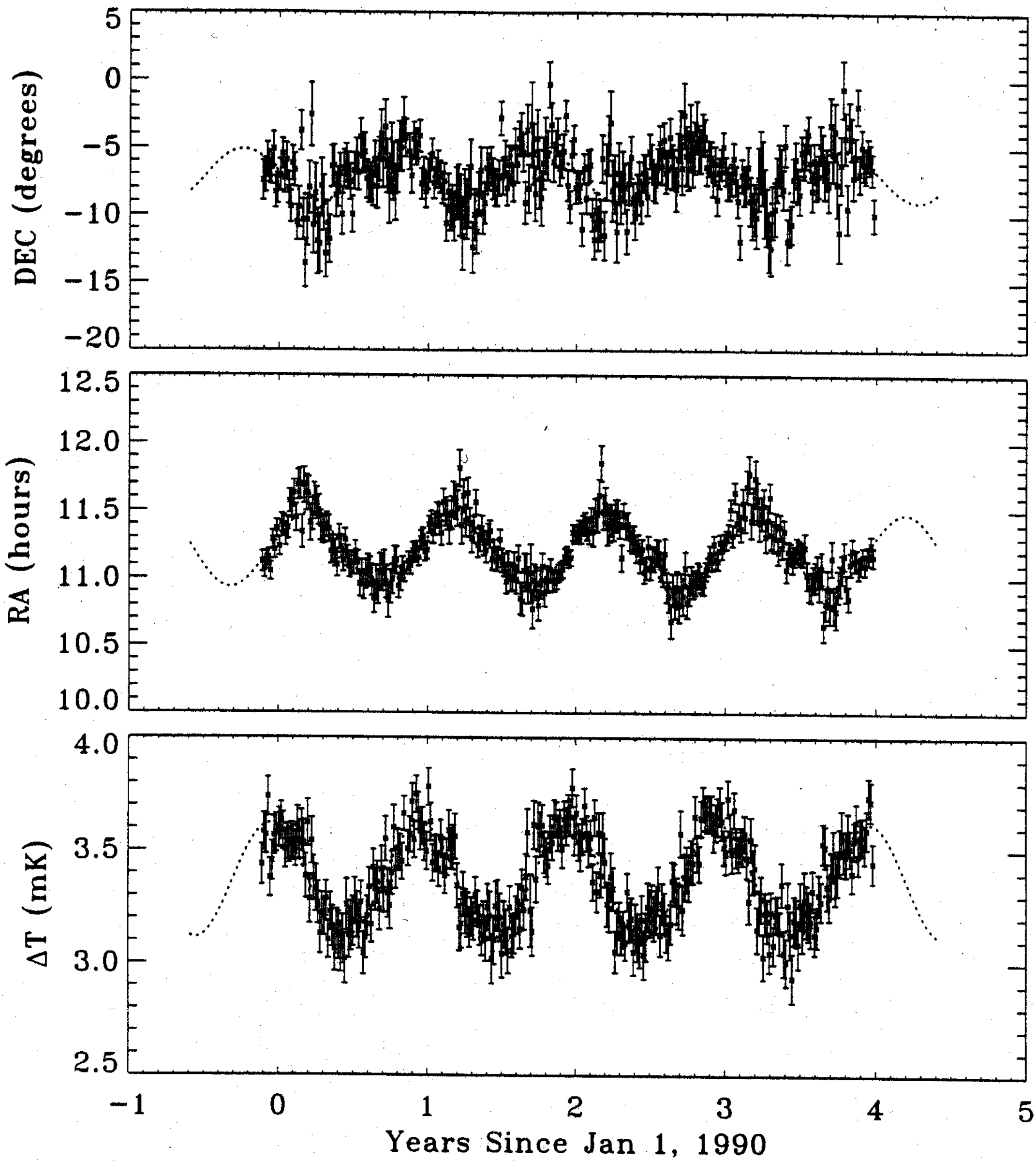

Figure 3: Modulation of the CMB dipole resulting from the Doppler effect of the Earth's orbital motion about the Sun (channel 53B). Each datum represents 5 days. The amplitude of the modulation provides an independent absolute calibration.

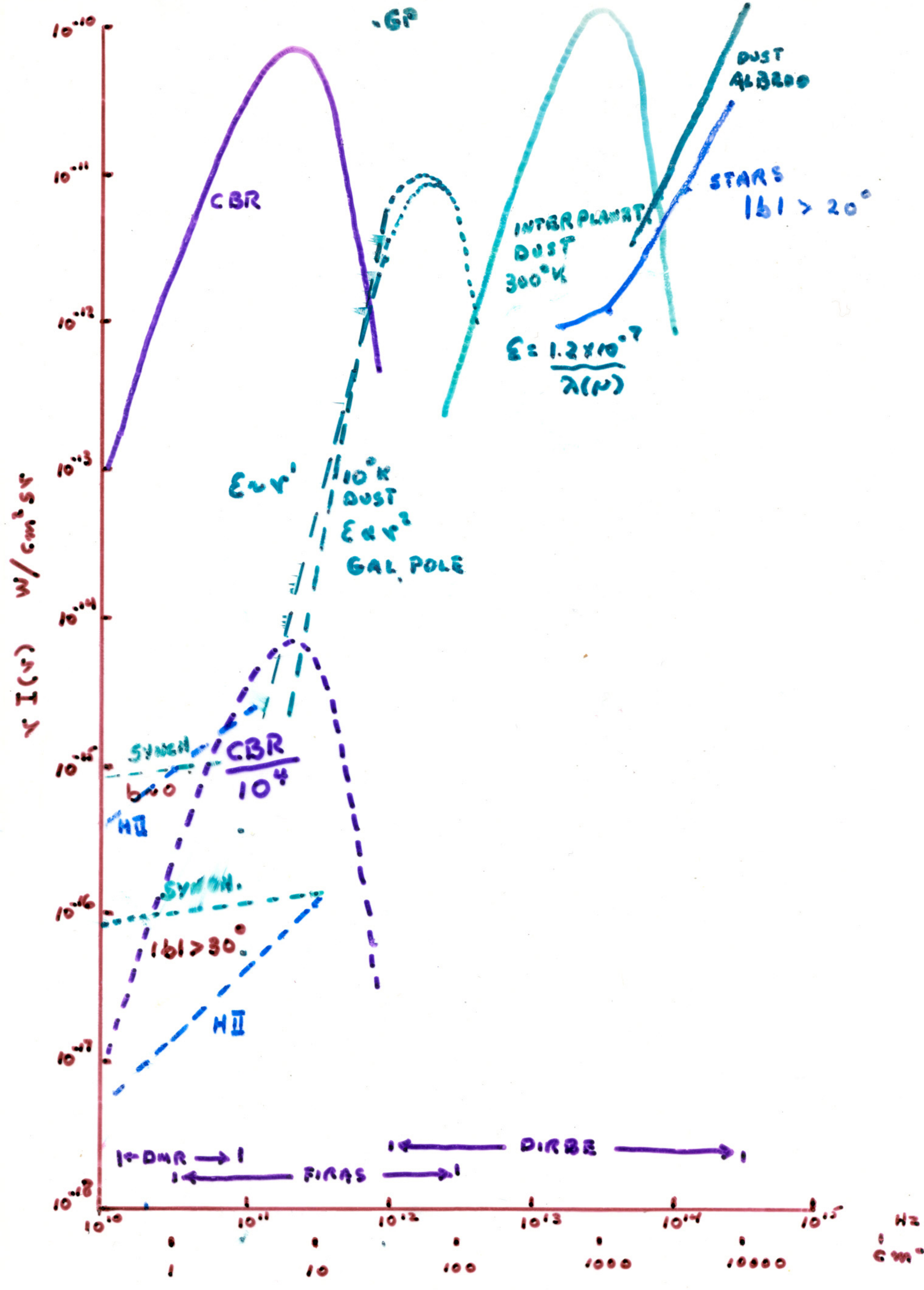

10^{-10}
10^{-11}
10^{-12}
10^{-13}
10^{-14}
10^{-15}
10^{-16}
10^{-17}
10^{-18}
$\nu I(\nu)$ W/cm² sr
.GP
CBR
DUST ALBEDO
STARS
$|b| > 20°$
INTERPLANET. DUST 300°K
$\epsilon = \frac{1.2 \times 10^{-7}}{\lambda(\mu)}$
$\epsilon \sim \nu^1$
10°K DUST
$\epsilon \propto \nu^2$
GAL. POLE
SYNCH
b=0
$\frac{CBR}{10^4}$
H II
SYNCH.
$|b| > 30°$
H II
DIRBE
DMR
FIRAS
10^{10}
10^{11}
10^{12}
10^{13}
10^{14}
10^{15}
Hz
1
10
100
1000
10000
cm^{-1}

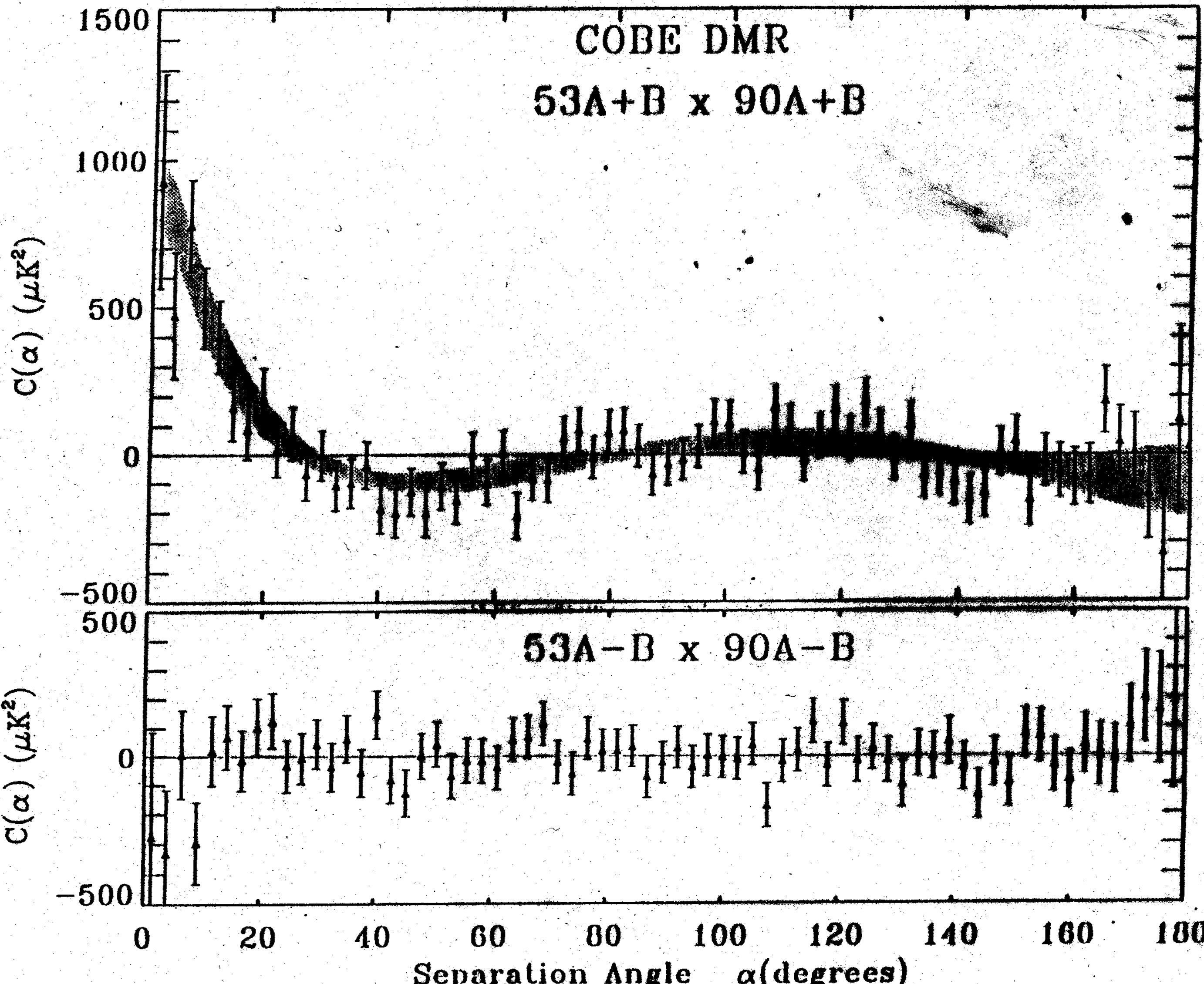

COBE DMR
53A+B x 90A+B
53A−B x 90A−B
C(α) (μK²)
C(α) (μK²)
1500
1000
500
0
−500
500
0
−500
0
20
40
60
80
100
120
140
160
180
Separation Angle α(degrees)

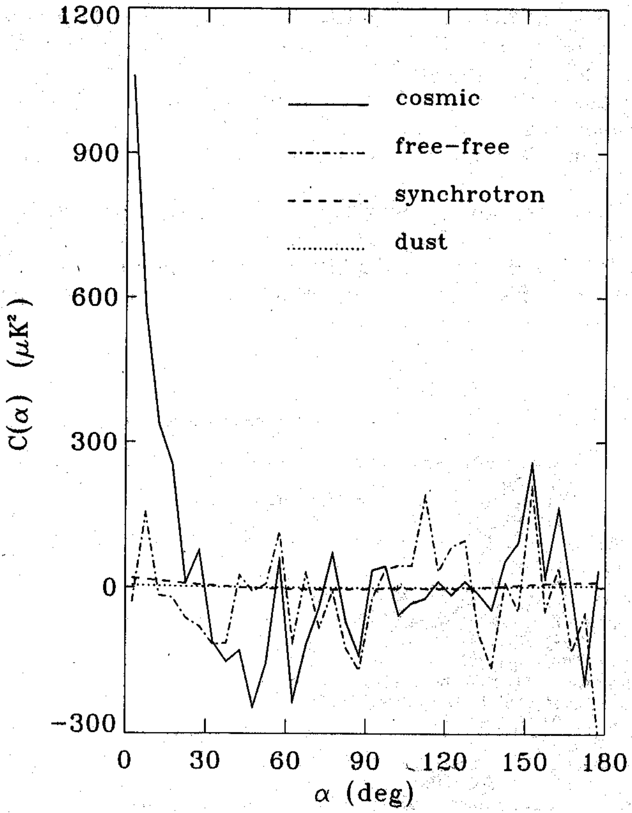

FIG. 4.—Autocorrelation functions for the Galactic and cosmic signals at 53 GHz from the subtraction technique are shown for $|b| > 20°$. The synchrotron and dust signals are weak. Smoot et al. (1992) show the autocorrelation function for the 53 GHz map with no Galactic signal removed. The removal of modeled Galactic emission leaves the autocorrelation function virtually unchanged. Instrument noise dominates the cosmic and free-free signals at large angular separations; since these signals are derived from the same DMR data, their noise is correlated.

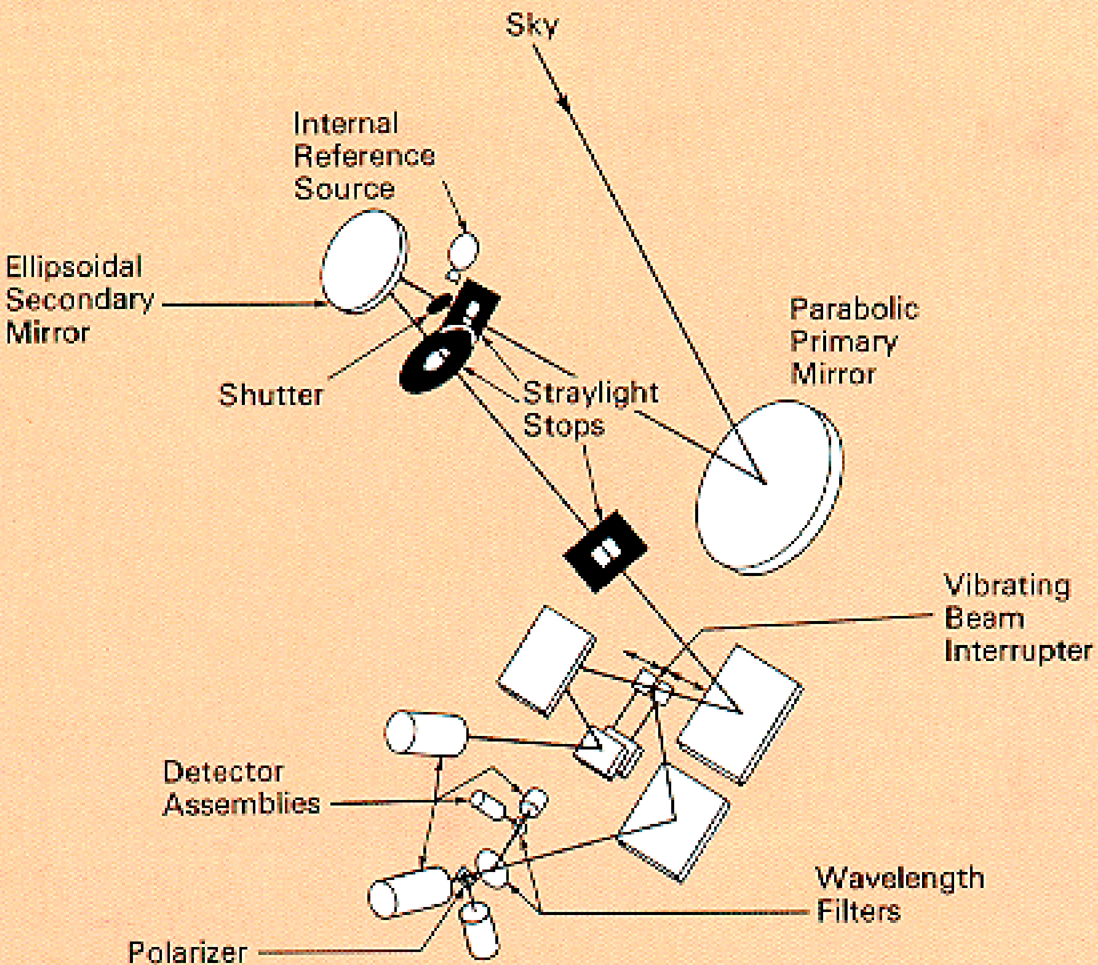
Sky
Internal Reference Source
Ellipsoidal Secondary Mirror
Parabolic Primary Mirror
Shutter
Straylight Stops
Vibrating Beam Interrupter
Detector Assemblies
Wavelength Filters
Polarizer

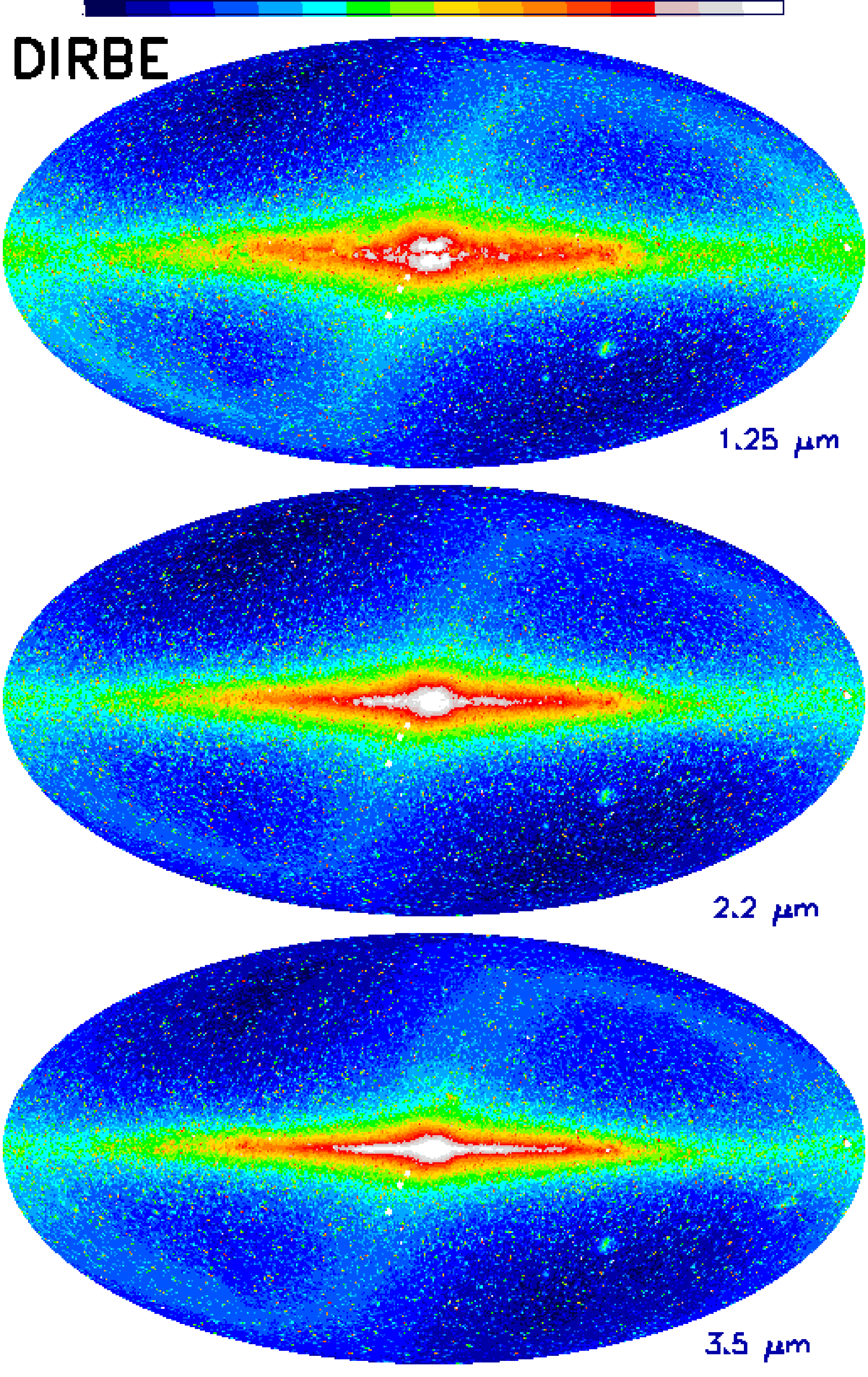

DIRBE
1.25 μm
2.2 μm
3.5 μm

DIRBE 1.25, 2.2, 3.5 μm Composite

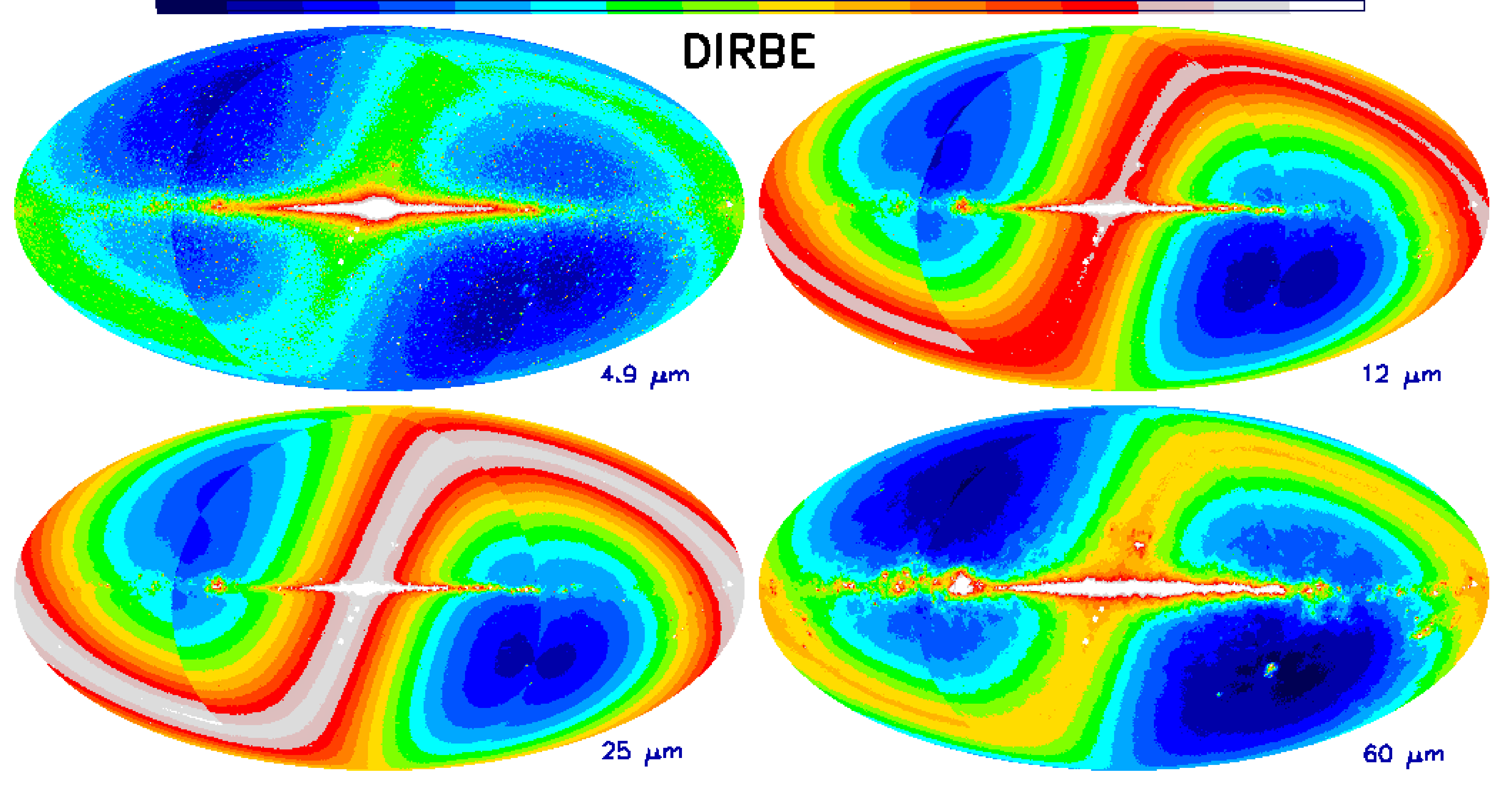
DIRBE
4.9 μm
12 μm
25 μm
60 μm

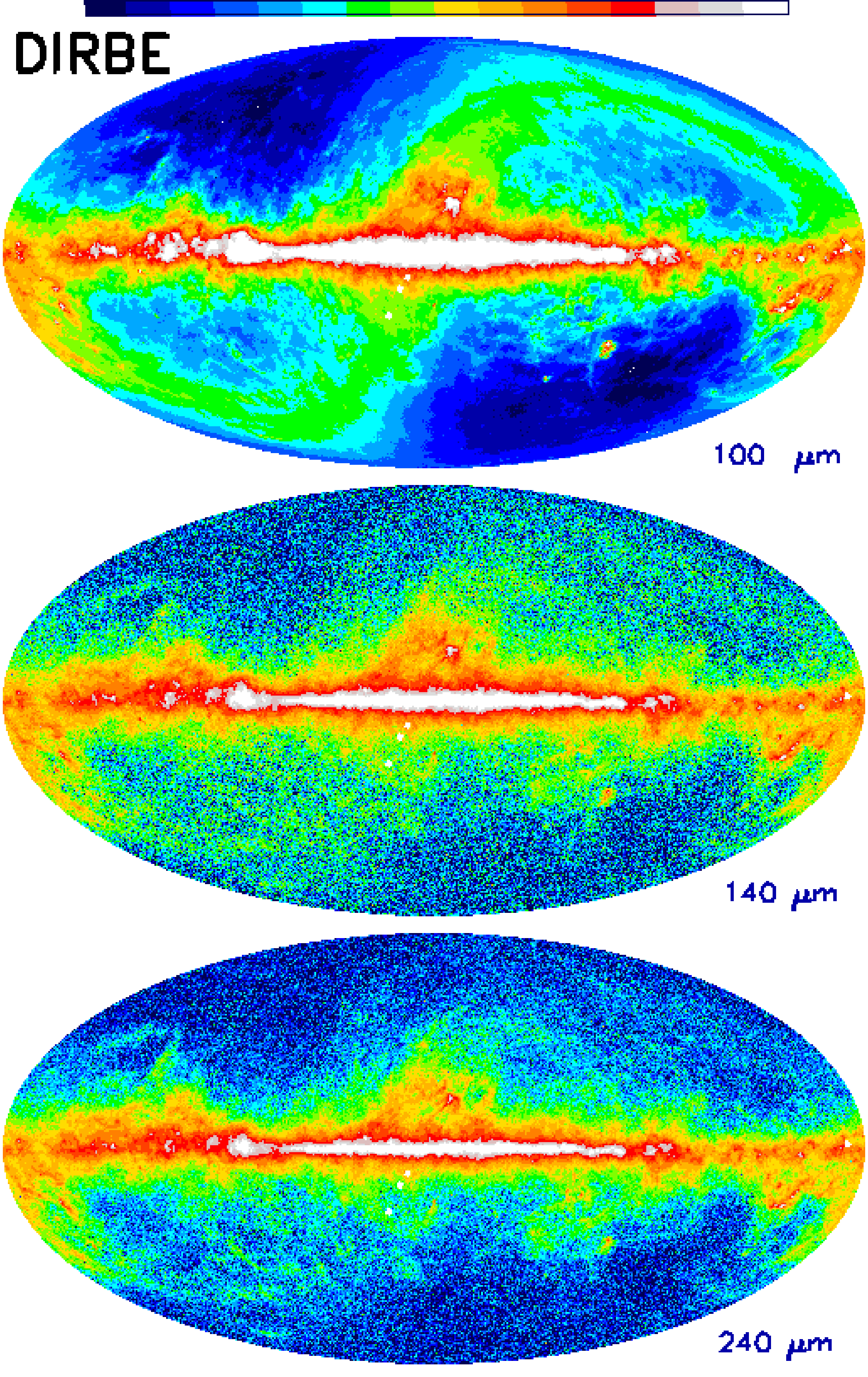
DIRBE
100 μm
140 μm
240 μm

COBE - DIRBE

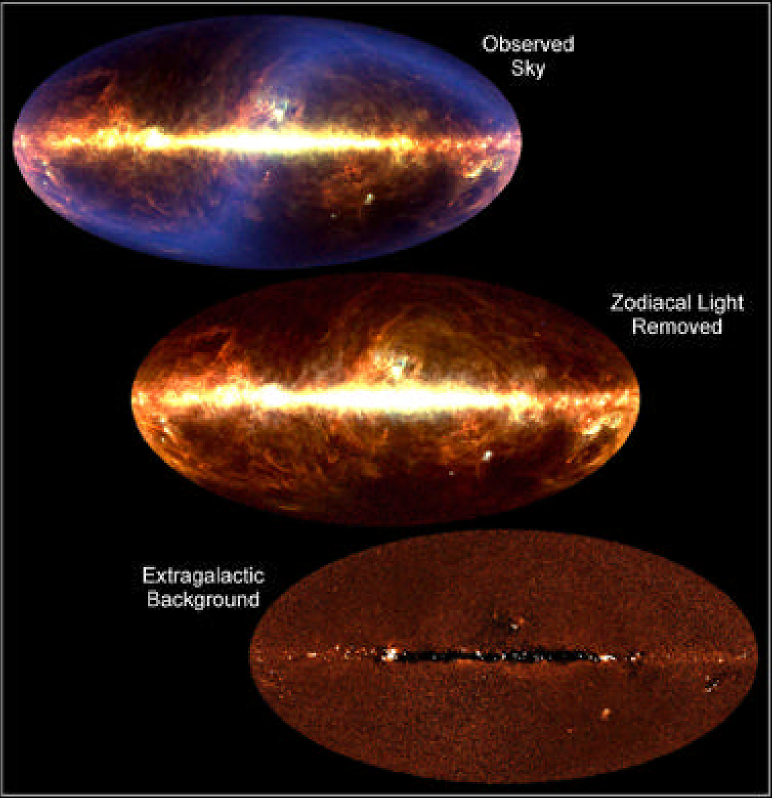
Observed Sky
Zodiacal Light Removed
Extragalactic Background

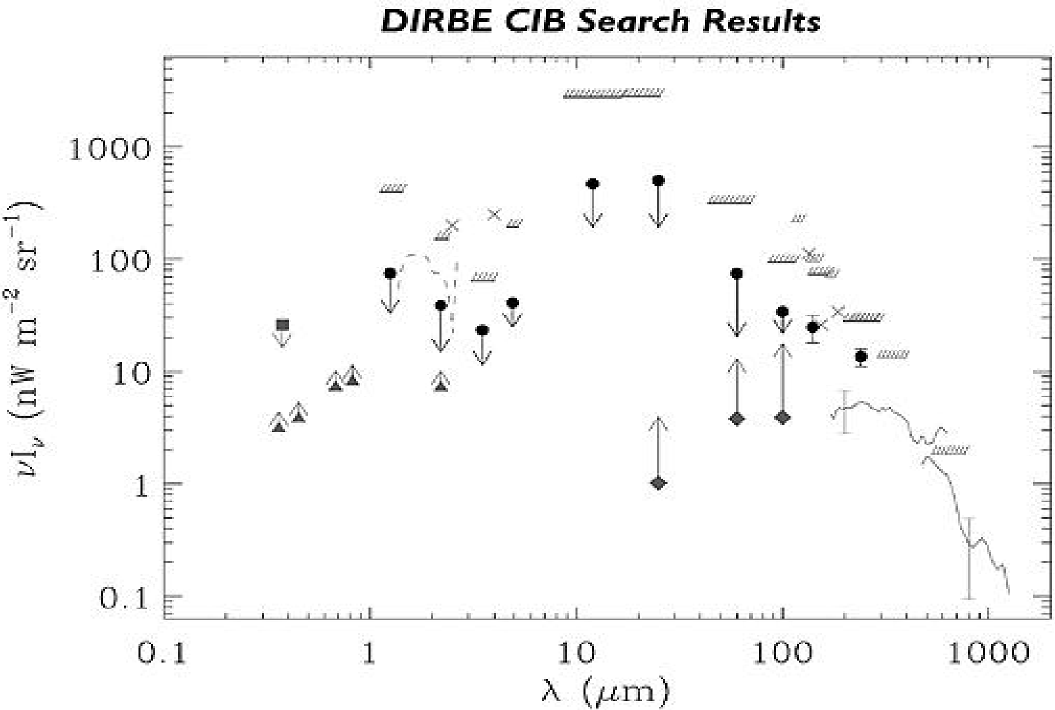
DIRBE CIB Search Results
1000
100
10
1
0.1
νI_ν (nW m^{-2} sr^{-1})
0.1
1
10
100
1000
λ (μm)